Revision 1

Rare Earth Perovskites along the $CaTiO_3$ - $Na_{0.5}La_{0.5}TiO_3$ join: Phase Transitions, Formation Enthalpies, and Implications for Loparite Minerals

Dawei Feng, Radha Shivaramaiah, and Alexandra Navrotsky*

Peter A. Rock Thermochemistry Laboratory and NEAT ORU, University of California Davis, Davis, CA 95616, USA

* Corresponding author. Tel.: (530) 752-3292; fax: (530) 752-9307.
E-mail address: anavrotsky@ucdavis.edu (A. Navrotsky).

Keywords: rare earth perovskites; calorimetry; enthalpy of formation; loparite.

Abstract

The mineral loparite is the principal ore of the light rare earth elements (LREE) with solid solution compositions in the quaternary system perovskite ($CaTiO_3$) - lueshite ($NaNbO_3$) - tausonite ($SrTiO_3$) - loparite ($Na_{0.5}Ln_{0.5}TiO_3$) (*Ln* =La, Ce, Pr, Nd). In this study, perovskite solid solutions $Ca_{1-2x}Na_xLa_xTiO_3$ ($0 \leq x \leq 0.50$) along the perovskite-loparite join were synthesized using solid state sintering methods. XRD analysis indicates that as the Na+La content increases, the structure changes from orthorhombic to tetragonal. The enthalpies of formation at 298 K from the constituent oxides ($\Delta H^{\circ}_{f,ox}$) and from the elements ($\Delta H^{\circ}_{f,el}$) have been determined using high temperature oxide melt solution calorimetry in molten $3Na_2O{\cdot}4MoO_3$ at 973 K. Enthalpy of formation from oxides $\Delta H^{\circ}_{f,ox}$ becomes more exothermic with increasing Na+La content, suggesting a stabilization effect of the substitution $Ca^{2+} \rightarrow 0.5Na^{+} + 0.5La^{3+}$. The observed trend of increasing thermodynamic stability with decreasing structural distortion is in agreement with that seen in many other ABO_3 perovskites. The thermodynamic stability of perovskite solid solutions $Ca_{1-2x}Na_xLa_xTiO_3$ ($0 \leq x \leq 0.50$) along the $CaTiO_3$-$Na_{0.5}La_{0.5}TiO_3$ join provides insights into the natural occurrence of loparite minerals (La, Na, Sr, Ca)(Ti, Nb, Ta, Fe^{3+})O_3.

Introduction

Loparite, a complex perovskite with general formula (Ce, Na, Sr, Ca) (Ti, Nb, Ta, Fe^{+3})O_3, is of significance ranging from mineralogy to advanced materials. From the geoscience point of view, the mineral loparite is the principal ore of the light rare-earth elements (LREE), found, for example, in Russia (Hedrick et al. 1997), Canada (Chakhmouradian et al. 2007; Platt 1994), South America (Haggerty and Mariano 1983) as well as the USA (Mitchell and Chakhmouradian 1999). It is a ubiquitous accessory mineral in agpaitic alkaline lithologies, with particular interest in petrogenetic investigations (Mitchell et al. 2011). Most recently, loparite-(Ce) has also been found with promising ferroelectric properties (Popova et al. 2014).

Loparite was first described by Wilhelm Ramsay in 1890 from the agpaitic syenites of the Lovozero alkaline complex in Kola Peninsula of Russia (Ramsay and Hackman 1894) and the chemical composition was analyzed later (Bykova 1941). Loparite belongs to the perovskite family where the *A*-site may accommodate alkali, alkaline earth and rare earth cations, ranging from monovalent to trivalent. The structure of loparite-(Ce) minerals has been determined (Mitchell et al. 2000a; Mitchell and Chakhmouradian 1996) using single crystal X-ray diffraction and is often described to have pseudocubic symmetry. Niobian calcian loparite-(Ce) from the Khibina complex in Russia has been found with orthorhombic structure, while calcian niobian loparite-(Ce) from the Lovozero complex in Russia and strontian calcian loparite-(Ce) from the Bearpaw Mountains in Montana are tetragonal.

Naturally occurring perovskites are of importance as indicators of geochemical evolution and as ores for rare earths. Loparite minerals, with the ideal end member chemical formula $Na_{0.5}Ln_{0.5}TiO_3$ (Ln = rare earth), belong to the perovskite group of rare earth minerals that also includes $CaTiO_3$ (perovskite), $NaNbO_3$ (lueshite) and $SrTiO_3$ (tausonite). Among naturally occurring perovskite titanates, the quaternary system $CaTiO_3$–$NaNbO_3$–$SrTiO_3$–$Na_{0.5}Ln_{0.5}TiO_3$ (Ln = La, Ce, Pr, Nd) represents much of the compositional variations. In many occurrences, a solid solution is found between $Na_{0.5}Ln_{0.5}TiO_3$ and other perovskite end members. Figure 1 depicts the quaternary system perovskite ($CaTiO_3$) - lueshite ($NaNbO_3$) - tausonite ($SrTiO_3$) - loparite ($Na_{0.5}Ln_{0.5}TiO_3$). There has been considerable research carried out within this quaternary system. Thermodynamic and crystal chemical properties of several constituent binary systems have been investigated, including tausonite ($SrTiO_3$) - loparite ($Na_{0.5}La_{0.5}TiO_3$) (Mitchell et al. 2000b), lueshite ($NaNbO_3$) - tausonite ($SrTiO_3$) (Xu et al. 2005), as well as perovskite ($CaTiO_3$) - tausonite ($SrTiO_3$) (Navi et al. 2012). Nevertheless, research on other rare earth containing perovskite mineral systems containing the loparite end member ($Na_{0.5}La_{0.5}TiO_3$) is still relatively scarce, particularly in terms of thermodynamic properties.

The solid solution $Ca_{1-2x}Na_xLa_xTiO_3$ ($0 \leq x \leq 0.50$) is an *A*-site substituted perovskite series between perovskite ($CaTiO_3$) and loparite ($Na_{0.5}La_{0.5}TiO_3$) end members. Structure of both the end members is shown in Figure 2. Synthetic $Na_{0.5}La_{0.5}TiO_3$ has been described structurally and is claimed to have the undistorted cubic perovskite structure with the space group $Pm\overline{3}m$, and La^{3+} and Na^{+} ions randomly distributed at the 12-fold cuboctahedral site (Brous et al. 1953). The crystal structure of the natural mineral loparite has also been determined as the cubic modification for the first time by X-ray diffraction analysis (Zubkova et al., 2000). In contrast, other studies showed that $Na_{0.5}La_{0.5}TiO_3$ may crystallize with either orthorhombic (*Pnma*) (Mitchell and Chakhmouradian 1998) or rhombohedral ($R\overline{3}c$) symmetry (Mitchell et al. 2000 b). These observed differences might be due to the different synthesis routes and/or slight variations in the Na/La ratio (Mitchell et al. 2000 b). The other end member in the $CaTiO_3$ - $Na_{0.5}La_{0.5}TiO_3$ series, $CaTiO_3$, has been studied extensively (e.g. Buttner and Maslen 1992; Sasaki et al. 1987). At room temperature, $CaTiO_3$ exhibits the orthorhombic space group *Pbnm*. This structure is derived from the $Pm\overline{3}m$ aristotype by octahedral tilting about the three four - fold axes of the cubic subcell. Phase transitions have been reported from the room temperature orthorhombic (Pbnm) structure to a tetragonal (I4/mcm) polymorph at temperatures in the range 1373 - 1423 K, followed by transformation to the cubic (Pm$\overline{3}$m) aristotype at 1523 ± 10 K (Guyot et al. 1993; Redfern et al. 1989).

In this study, we synthesized the $CaTiO_3$ - $Na_{0.5}La_{0.5}TiO_3$ rare earth perovskites solid solution by solid state reaction. We analyzed structures of the intermediate members in the series by X-ray powder diffraction with particular emphasis on the phase transition and changes in symmetry. One purpose of this study is, therefore, to obtain more insights into the structures and the influence of the *A*-site substitution on the phase transition. Another goal is to determine thermodynamic properties in the system $Ca_{1-2x}Na_xLa_xTiO_3$ ($0 \leq x \leq 0.5$) by measuring heats of formation using high temperature oxide melt solution calorimetry. The energetics of these substitutions could help understand the A-site substitutions and the occurrences of these rare earth perovskite minerals in nature as well as their processing as ores of rare earths and niobium.

Experimental Methods

Materials

Powder samples in the system, $Ca_{1-2x}Na_xLa_xTiO_3$ ($0 \leq x \leq 0.5$), were made from stoichiometric amounts of $CaCO_3$, Na_2CO_3, TiO_2 and La_2O_3 by standard solid state synthesis. The reagents were dried for 5 hours at 1273 K for TiO_2 (Aldrich 99.99%), 773 K for $CaCO_3$ (Alfa Aesar 99.9%), 1273 K for La_2O_3 (Alfa Aesar 99.9%), and 423 K for Na_2CO_3 (Alfa Aesar 99.9%). Stoichiometric mixtures with the addition of 2 wt % excess Na_2CO_3 (to compensate for sodium vaporized at high temperature) were mixed and ground in an agate mortar, then heated in air initially from 773 K to 1073 K at 30 K/h, held at this temperature for 12 h, and then cooled to ambient. After grinding in an agate mortar, the samples were fired again in air at 1473 K for at least 72 h with periodic regrinding, finally rapidly cooled in air to room temperature. The calcined powder was cold pressed and sintered at 1473 K for 12 h. The sintered pellets were crushed and annealed at 973 K for diffraction and calorimetric experiments.

Characterization

Room temperature powder X-ray diffraction (XRD) of the synthesis products was carried out on a Bruker D8 diffractometer (Bruker-AXS Inc., Madison WI) operated at an accelerating voltage of 40 kV and an emission current of 40 mA with a rotating sample stage using CuK_α radiation (λ = 0.15406 nm). Data were recorded between 20 and 130 ° 2θ with steps of 0.02 ° and counting time of 10 s per step. XRD data were then analyzed using the Rietveld method with GSAS software. Refined parameters were background coefficients, histogram scale factors, lattice parameters and profile parameters.

The chemical compositions were analyzed using wavelength dispersive electron probe microanalysis using a Cameca SX100 instrument (Cameca Inc., Gennevilliers, France) on polished samples. The instrument was operated at an accelerating voltage of 15 kV, with a 20 nA beam current and a spot size of 1 μm. The compositions were calculated from an average of 10 data points per sample. The standards used were $NaAlSi_3O_8$ (albite), $LaPO_4$, CaO and TiO_2.

Calorimetry

High temperature drop solution calorimetry in molten sodium molybdate ($3Na_2O\cdot4MoO_3$) at 973 K was performed in a custom built Tian - Calvet twin calorimeter. The details of the calorimeter and methodology have been described previously (Navrotsky 1977; 1997; 2014). Prior to calorimetry, compounds were stored in a desiccator. For each measurement, a ~5 mg pellet was loosely pressed, weighed on a microbalance and dropped from room temperature into $3Na_2O\cdot4MoO_3$ melt at 973 K. The calorimeter was calibrated using the heat content of corundum. Oxygen was bubbled through the solvent at 5 ml/min and flushed over it at 50 ml/min to stir the melt and retain oxidizing conditions. The methodology was the same as that used in our laboratory for other perovskites (Xu et al. 2005; Feng et al. 2016).

Results

Structure and chemical analysis

The formation of a phase with perovskite structure was confirmed by XRD for all samples and no secondary phases were detected. Sodium deficit has been observed in high temperature synthesis of sodium compounds, resulting from the fact that Na_2CO_3 could decompose into Na_2O and CO_2 at 851 C. The vapor pressure of Na_2O is relatively high (Brewer and Margrave, 1955), which could explain the sodium deficit. A systematic Na deficit was found in initial syntheses using nominally stoichiometric mixtures of reagents. The addition of 2 wt % excess Na_2CO_3 to compensate for sodium vaporized at high temperatures gave good final chemical compositions as seen from Table 1. From the microprobe analysis, the chemical compositions were found to be close to nominal with a systematic Na deficit on the order of 1 % (which is within experimental error of the nominal composition) and homogeneity at the 2 % level. Figure 3 shows X-ray diffraction data and calculated patterns for $Ca_{1-2x}Na_xLa_xTiO_3$ ($0 \leq x \leq 0.50$). All the phases were perovskites with rhombohedral or tetragonal symmetry. In ABO_3 perovskites, structural distortions from the ideal $Pm\overline{3}m$ aristotype can often be described in terms of tilting of rigid BO_6 octahedra. Structure models for the Rietveld refinements for the end members are taken from the literature (Li et al. 2007). For the solid solutions, the LeBail fit was done using both *Pbnm* and *I4/mcm* space groups and the ones with the lowest goodness of fit parameters were chosen for the Rietveld refinements. Since there is no long range cation ordering in these materials, all three cations (La, Na, Ca) were assumed to be distributed randomly in the A-site. With increasing sodium and lanthanum content, a transition from orthorhombic *Pbnm* to tetragonal *I*4/*mcm* structure was observed. The cell parameters obtained from the refinements of the entire solid solution are listed in Table 1 and plotted in Figure 4. The cell edge lengths *a* and *b* of the *Pbnm* phase converge near x = 0.375 with increasing *x*, indicating a phase transformation to the tetragonal *I*4/*mcm* phase at this composition.

Enthalpies of formation

The measured enthalpies of drop solution, ΔH_{ds}, of $Ca_{1-2x}Na_xLa_xTiO_3$ ($0 \leq x \leq 0.50$) were used for determination of the enthalpy of formation from binary oxides, $\Delta H_{f,ox}$, and from elements, $\Delta H_{f,el}$. Table 2 shows the thermochemical cycles used for the calculation of formation enthalpies of $Ca_{1-2x}Na_xLa_xTiO_3$ (0

$\leq x \leq 0.50$) from binary oxides and from elements. The results on enthalpies of rare earth perovskites $Ca_{1-2x}Na_xLa_xTiO_3$ ($0 \leq x \leq 0.50$) at 298 K are summarized in Table 3. The drop solution enthalpies as a function of composition are shown in Figure 5.

Discussion

The powder XRD analysis at room temperature confirms a phase transition in $Ca_{1-2x}Na_xLa_xTiO_3$ ($0 \leq x \leq 0.50$) solid solutions. With increasing sodium and lanthanum content, a phase transition from orthorhombic *Pbnm* to tetragonal *I*4/*mcm* structure has been observed. Other A-site substituted perovskite solid solutions show analogous transformations. For example, in the tausonite ($SrTiO_3$) - lueshite ($NaNbO_3$) series, the structures of the perovskite solid solution $Na_{1-x}Sr_xNb_{1-x}Ti_xO_3$ ($0 \leq x \leq 1$) change from orthorhombic to tetragonal and finally to cubic (Xu et al. 2005). In the tausonite ($SrTiO_3$)-loparite ($Na_{1/2}La_{1/2}TiO_3$) series, the structures of the solid solution $Sr_{1-2x}Na_xLa_xTiO_3$ ($0 \leq x \leq 0.50$) change from cubic to tetragonal and finally to rhombohedral (Mitchell et al. 2000b). In the perovskite ($CaTiO_3$) - tausonite ($SrTiO_3$) series, the structures of solid solutions $Ca_xSr_{1-x}TiO_3$ ($0 \leq x \leq 1$) change from orthorhombic to tetragonal (Navi et al. 2012). As mentioned above, the commonly accepted space group for the end-member $Na_{1/2}La_{1/2}TiO_3$ seems to be tetragonal *I*4/*mcm* (Li et al. 2007), not the rhombohedral $R\overline{3}c$ reported by Mitchell et al. (2000a). Our structure refinements confirm this as well. Both *Pbnm* to *I*4/*mcm* and *Pbnm* to $R\overline{3}c$ transitions are of first order (Howard and Stokes 1998). Although the transition from *Pbnm* directly to $R\overline{3}c$ has been observed in some cases, such as the *B*-site substituted perovskites in the $LaNiO_3$–$LaFeO_3$ system (Falcon et al. 1997), and the *A*- and *B*-site substituted perovskites in the $LaCrO_3$–$SrTiO_3$ series (Kennedy et al. 2000), it has not been reported in *A*-site substituted perovskites.

The enthalpy of formation of $Ca_{1-2x}Na_xLa_xTiO_3$ ($0 \leq x \leq 0.50$) from the oxides is plotted in Figure 6(a). With increasing Na+La substitution at the A site, the enthalpy of formation becomes more exothermic, implying greater stability relative to the binary oxides. The distortion from cubic symmetry can be rationalized using the Goldschmidt tolerance factor, $t = (r_A + r_O)/\sqrt{2}(r_B + r_O)$ (Goldschmidt 1926). Figure 6(b) shows a linear trend between the enthalpy of formation and the Goldschmidt tolerance factor, consistent with previous trends in perovskite stability (Navrotsky 2000; Xu et al. 2005; Zlotnik et al. 2015). Interestingly, there is no change in slope near the phase transformation (space group change), suggesting that the enthalpy of the phase transition is small, probably 1 kJ/mol or less, as seen in other perovskites (Navrotsky 2000; Xu et al. 2005; Zlotnik et al. 2015).

XRD analysis indicates that as the Na+La content increases, the structure changes from orthorhombic to tetragonal near x = 0.375. The formation enthalpies from oxides ($\Delta H^{\circ}_{f,ox}$) become more exothermic with increasing Na+La content, suggesting a stabilization effect of the substitution $Ca^{2+} \rightarrow 0.5Na^{+} + 0.5\ La^{3+}$. The trend of increasing thermodynamic stability with decreasing structural distortion is consistent with that seen in many other ABO_3 perovskites, reflecting increasing stability as the tolerance factor approaches unity.

Implications

Natural loparite minerals occur as perovskite solid solutions, mainly in the quaternary system perovskite ($CaTiO_3$) - lueshite ($NaNbO_3$) - tausonite ($SrTiO_3$) - loparite ($Na_{1/2}Ln_{1/2}TiO_3$) (*Ln* =La, Ce, Pr, Nd) (see Figure 1). It is interesting to compare the energetics of the various substitutions along these joins. The substitution along the $CaTiO_3$-$Na_{0.5}La_{0.5}TiO_3$ join can be written as the following,

$$Ca^{2+} \leftrightarrow 0.5\ Na^{+} + 0.5\ La^{3+} \qquad (1)$$

which can also be written, in terms of oxide components

$$CaTiO_3 + 0.25Na_2O + 0.25La_2O_3 = Na_{0.5}La_{0.5}TiO_3 + CaO. \qquad (2)$$

Since there is negligible enthalpy of mixing along this solid solution, one can take the difference in enthalpy of formation of the end members as the enthalpy of the substitution, namely $\Delta H = \Delta H_{f,ox}$

($Na_{0.5}La_{0.5}TiO_3$) - $\Delta H_{f,ox}$ ($CaTiO_3$) = -16.0 kJ/mol. Xu et al. (2005) investigated the energetics of perovskite solid solutions along the $NaNbO_3$-$SrTiO_3$ join and found that the formation enthalpy becomes more exothermic with increasing Na+Nb content, suggesting stabilization with respect to component oxides for the substitution,

$$Sr^{2+} + Ti^{4+} \leftrightarrow Na^{+} + Nb^{5+} \quad (3)$$

or, relative to oxide components,

$$SrTiO_3 + 0.5\ Na_2O + 0.5\ Nb_2O_5 = NaNbO_3 + SrO + TiO_2 \quad (4)$$

Again, with an observed negligible heat of mixing along the solid solution $\Delta H = \Delta H_{f,ox}$ ($NaNbO_3$) - $\Delta H_{f,ox}$ ($SrTiO_3$) = -40.3 kJ/mol. The energetics of other substitutions, calculated analogously from the differences in enthalpies of formation of end member perovskites, are shown in Table 4. The stabilizing effect, relative to binary oxides, of the sodium-containing substitutions reflects the greater basicity of Na_2O than of CaO or SrO. The substitution of Na + La is energetically favorable for Ca but not for Sr. Since the alkali and alkaline earth ions can only occupy the A-sites, the maximum extent of substitution depends on whether the charge balancing cation of higher valence occupies A-sites (like the rare earths) or the B-sites (like niobium), with greater substitution possible in the latter case (compare $Na_{0.5}La_{0.5}TiO_3$ and $NaNbO_3$ as end members). The stabilizing effect of the substitution of Sr for Ca reflects the greater basicity of SrO than CaO. The Na + Nb substitution is more stabilizing than the Na + La substitution.

These energetic trends can be compared to substitution patterns seen in natural loparite minerals. The compositions of loparite(Ce) from the layered complex at Lovozero, Russia (Pakhomovsky et al. 2014) generally follow the schemes of isomorphic replacements. The loparites, though variable in composition, fall in a relatively narrow composition range, with factor analysis suggesting the following two major substitutions: $2Ca^{2+} + Ti^{4+} = Sr^{2+} + Na^{+} + Nb^{5+}$ at constant rare earth content and $Ln^{3+} + Ti^{4+} = Ca^{2+} + Nb^{5+}$ at constant Na and Sr contents. These are indeed energetically stabilizing substitutions as can be calculated from the data in Table 4. Suk et al. (2013) studied loparite from a complex of differentiated rocks and from the Lovozero alkaline massif. They also carried out experimental studies of loparite formation in complex silicate - molten salt systems including sodium carbonate, chloride, fluoride, and sulfate at 673 –1473 K and 1–2 kbar. The results show that the composition of loparites depends on the physicochemical conditions of their formation (fluid/melt composition) and that loparite can crystallize in a wide range of temperatures. The synthetic loparite crystals are zoned with variations in Ti, Nb, La, Ce, Y, Ca, and Sr contents and are similar to those in the natural systems. Higher alkalinity of the fluid appears to initially favor loparite formation. This is in accord with the thermochemical data in Table 4 which show that the Na + Ca and Na + Nb substitutions are energetically favorable. Kogarko et al. (2002) observed that the composition of the cumulus loparite changes systematically upwards through the Lovozero intrusion with an increase in Na, Sr, Nb and Th and decrease in REE and Ti. At later stages of evolution, when concentrations of alkalis and volatiles in the fluid reached very high levels, loparite reacted with the residual melt to form a variety of other minerals incorporating rare earths. From our research, we found that the synthesis of sodium rich compounds ($x > 0.5$) in the $Ca_{1-2x}Na_xLa_xTiO_3$ was not successful. We could conclude that the $Ca^{2+} \leftrightarrow 0.5Na^+ + 0.5Ln^{3+}$ substitution is complete at $x = 0.5$ when the A site is completely substituted. This substitution is in competition with the $Ca^{2+} + Ti^{4+} = Na^+ + Nb^{5+}$ substitution. Again, since sodium can only enter the A-site, the ability of perovskite to accommodate Na + Nb may become limited at very high alkalinity. Therefore additional sodium, niobium, and lanthanum concentrations in the reacting medium would have to react to form other compounds, as is observed.

Acknowledgements

This work was supported by the National Science Foundation, Division of Earth Sciences with contributions from the NSF-wide SUSchem initiative (grant EAR- 1321410).

References

Brewer, L., and Margrave, J. (1955) The Vapor Pressures of Lithium and Sodium Oxides. Journal of Physical Chemistry, 59(5), 421-425.

Brous, J., Fankuchen, I., and Banks, E. (1953) Rare Earth Titanates with a Perovskite Structure. Acta Crystallographica*,* 6 (1), 67-70.

Buttner, R. H., and Maslen, E. N. (1992) Electron Difference Density and Structural Parameters in $CaTiO_3$. Acta Crystallographica B*,* 48, 644-649.

Bykova, V.S. (1941) Chemical Composition of the Lovozero Loparite and a Method for its Analysis. Proceedings of the USSR Academy of Sciences, 33(2), 136-139.

Chakhmouradian, A.R., Halden, N.M., Mitchell, R.H., and Horvath, L. (2007) Rb-Cs-rich Rasvumite and sector-zoned "Loparite-(Ce)" from Mont Saint-Hilaire (Quebec, Canada) and their petrologic Significance. European Journal of Mineralogy, 19(4), 533-546.

Chase, M.W., Jr. (1998) NIST-JANAF Themochemical Tables. 1-1951 p. American Chemical Society, Woodbury, N.Y.

Cheng, J.J., Navrotsky, A., Zhou, X.D., and Anderson, H.U. (2005) Thermochemistry of $La_{1-x}Sr_xFeO_{3-\delta}$ solid solutions ($0.0 \leqslant x \leqslant 1.0$, $0.0 \leqslant \delta \leqslant 0.5$). Chemistry of Materials, 17(8), 2197-2207.

Falcon, H., Goeta, A. E., Punte, G., and Carbonio, R. E. (1997) Crystal structure refinement and stability of $LaFe_xNi_{1-x}O_3$ solid solutions. Journal of Solid State Chemistry, *133* (2), 379-385

Feng, D., Maram, P.S., Mielewczyk, A., and Navrotsky, A. (2016) Thermochemistry of Rare Earth Perovskites $Na_{3x}RE_{0.67-x}TiO_3$ (RE = La, Ce). American Mineralogist, in press. DOI: http://dx.doi.org/10.2138/am-2016-5529

Goldschmidt, V.M. (1926) Die Gesetze der Krystallochemie. Die Naturwissenschaften, 21, 477–485.

Guyot, F., Richet, P., Courtial, P., and Gillet, P. (1993) High-Temperature Heat-Capacity and Phase-Transitions of $CaTiO_3$ Perovskite. Physics and Chemistry of Minerals, 20(3), 141-146.

Haggerty, S.E., and Mariano, A.N. (1983) Strontian-Loparite and Strontio-Chevkinite - 2 New Minerals in Rheomorphic Fenites from the Parana Basin Carbonatites, South America. Contributions to Mineralogy and Petrology, 84(4), 365-381.

Hedrick, J.B., Sinha, S.P., and Kosynkin, V.D. (1997) Loparite, a Rare-earth Ore (Ce, Na, Sr, Ca)(Ti, Nb, Ta, Fe^{+3})O_3. Journal of Alloys and Compounds, 250(1-2), 467-470.

Howard, C. J., and Stokes, H. T. (1998) Group-theoretical analysis of octahedral tilting in perovskites. Acta Crystallographica B 1998**,** *54*, 782-789.

Kennedy, B. J., Howard, C. J., Thorogood, G. J., Mestre, M. A. T., and Hester, J. R. (2000) Structural characterization of the perovskite series $La_{1-x}Sr_xCr_{1-x}Ti_xO_3$. Journal of Solid State Chemistry, 155 (2), 455-457.

Kogarko, L.N., Williams, C.T., and Woolley, A.R. (2002) Chemical Evolution and petrogenetic Implications of Loparite in the Layered, Agpaitic Lovozero Complex, Kola Peninsula, Russia. Mineralogy and Petrology, 74(1), 1-24.

Li, Y., Qin, S., and Seifert, F. (2007) Phase Transitions in A-site Substituted Perovskite Compounds: The $(Ca_{1-2x}Na_xLa_x)TiO_3$ $(0 \leq x \leq 0.5)$ Solid Solution. Journal of Solid State Chemistry, 180(3), 824-833.

Mitchell, R.H., Burns, P.C., and Chakhmouradian, A.R. (2000a) The Crystal Structures of Loparite-(Ce). Canadian Mineralogist, 38, 145-152.

Mitchell, R.H., and Chakhmouradian, A.R. (1996) Compositional Variation of Loparite from the Lovozero Alkaline Complex, Russia. Canadian Mineralogist, 34, 977-990.

-. (1998) A structural study of the perovskite series $Na_{1/2+x}La_{1/2-3x}Th_{2x}TiO_3$. Journal of Solid State Chemistry, 138 (2), 307-312.

-. (1999) Sr-bearing Perovskite and Loparite from Lamproite and Agpaitic Nepheline Syenite Pegmatites. Canadian Mineralogist, 37, 99-112.

Mitchell, R.H., Chakhmouradian, A.R., and Woodward, P.M. (2000b) Crystal Chemistry of Perovskite-type Compounds in the Tausonite-Loparite Series, $(Sr_{1-2x}Na_xLa_x)TiO_3$. Physics and Chemistry of Minerals, 27(8), 583-589.

Mitchell, R.H., Wu, F.Y., and Yang, Y.H. (2011) In situ U-Pb, Sr and Nd Isotopic Analysis of Loparite by LA-(MC)-ICP-MS. Chemical Geology, 280(1-2), 191-199.

Navi, N.U., Shneck, R.Z., Shvareva, T.Y., Kimmel, G., Zabicky, J., Mintz, M.H., and Navrotsky, A. (2012) Thermochemistry of $(Ca_xSr_{1-x})TiO_3$, $(Ba_xSr_{1-x})TiO_3$, and $(Ba_xCa_{1-x})TiO_3$ Perovskite solid Solutions. Journal of the American Ceramic Society, 95(5), 1717-1726.

Navrotsky, A. (1977) Progress and New Directions in High-Temperature Calorimetry. Physics and Chemistry of Minerals, 2(1-2), 89-104.

-. (1997) Progress and new Directions in High Temperature Calorimetry Revisited. Physics and Chemistry of Minerals, 24(3), 222-241.

-. (2000) Thermochemistry of Complex Perovskites. Fundamental Physics of Ferroelectrics 2000, 535, 288-296.

-. (2014) Progress and New Directions in Calorimetry: A 2014 Perspective. Journal of the American Ceramic Society, 97(11), 3349-3359.

Pakhomovsky, Y.A., Ivanyuk, G.Y., and Yakovenchuk, V.N. (2014) Loparite-(Ce) in Rocks of the Lovozero Layered Complex at Mt. Karnasurt and Mt. Kedykvyrpakhk. Geology of Ore Deposits, 56(8), 685-698.

Platt, R.G. (1994) Perovskite, Loparite and Ba-Fe Hollandite from the Schryburt Lake Carbonatite Complex, Northwestern Ontario, Canada. Mineralogical Magazine, 58(390), 49-57.

Popova, E.A., Zalessky, V.G., Yakovenchuk, V.N., Krivovichev, S.V., and Lushnikov, S.G. (2014) Ferroelectric Phase Transition and Relaxor-Like Behavior of Loparite-(Ce). Ferroelectrics, 469(1), 130-137.

Ramsay, W., and Hackman, V. (1894) Das Nephelinsyenitgebiet auf der Halbinsel Kola. Fennia, 14.

Redfern, S.A.T., Salje, E., and Navrotsky, A. (1989) High-Temperature Enthalpy at the Orientational Order-Disorder Transition in Calcite - Implications for the Calcite-Aragonite Phase-Equilibrium. Contributions to Mineralogy and Petrology, 101(4), 479-484.

Sasaki, S., Prewitt, C. T., Bass, J. D., and Schulze, W. A. (1987) Orthorhombic Perovskite $CaTiO_3$ and $CdTiO_3$ - Structure and Space Group. Acta Crystallographica C**,** 43, 1668-1674.

Suk, N.I., Kotel'nikov, A.R., and Viryus, A.A. (2013) Crystallization of Loparite in alkaline fluid-Magmatic Systems (from Experimental and Mineralogical Data). Russian Geology and Geophysics, 54(4), 436-453.

Tessier, F., Le Sauze, A., Marchand, R., and Navrotsky, A. (1999) Energetics of Nitridophosphates PON and "LiNaPON Glasses". Solid-State Chemistry of Inorganic Materials, 547, 389-394.

Xu, H.W., Navrotsky, A., Su, Y.L., and Balmer, M.L. (2005) Perovskite solid Solutions along the $NaNbO_3$-$SrTiO_3$ Join: Phase Transitions, Formation Enthalpies, and Implications for General Perovskite Energetics. Chemistry of Materials, 17(7), 1880-1886.

Zlotnik, S., Sahu, S.K., Navrotsky, A., and Vilarinho, P.M. (2015) Pyrochlore and Perovskite Potassium Tantalate: Enthalpies of Formation and Phase Transformation. Chemistry-a European Journal, 21(13), 5231-5237.

Zubkova, N.V., Arakcheeva, A.V., Pushcharovskii, D.Y., Semenov, E.I., and Atencio, D. (2000) Crystal structure of loparite. Crystallography Reports, 45(2), 210-214.

Table 1: Lattice parameters and space groups of $Ca_{1-2x}Na_xLa_xTiO_3$ perovskites ($0 \leq x \leq 0.5$)

Nominal Composition	Chemical Composition [a]	*a* (Å)	*b* (Å)	*c* (Å)	*Space group*
$Na_{0.5}La_{0.5}TiO_3$	$Na_{0.495}La_{0.5}TiO_{2.998}$	5.4769(3)	5.4769(5)	7.7539(3)	I4/mcm
$Ca_{0.25}Na_{0.375}La_{0.375}TiO_3$	$Ca_{0.25}Na_{0.371}La_{0.375}TiO_{2.998}$	5.4621(0)	5.4621(9)	7.7333(1)	I4/mcm
$Ca_{0.5}Na_{0.25}La_{0.25}TiO_3$	$Ca_{0.5}Na_{0.248}La_{0.25}TiO_{2.999}$	5.4302(3)	5.4580(5)	7.6926(3)	Pbnm
$Ca_{0.75}Na_{0.125}La_{0.125}TiO_3$	$Ca_{0.75}Na_{0.124}La_{0.125}TiO_{2.999}$	5.3979(2)	5.4527(2)	7.6409(3)	Pbnm
$CaTiO_3$	$CaTiO_3$	5.3765(2)	5.4286(2)	7.6261(4)	Pbnm

a. Composition analyzed by electron microprobe, considered to agree with nominal composition within experimental error.

Table 2. Thermochemical cycles for the calculation of formation enthalpies of $Ca_{1-2x}Na_xLa_xTiO_3$ ($0 \leq x \leq 0.50$) from binary oxides

Reactions	ΔH, kJ/mol
(a) Enthalpy of formation of $Ca_{1-2x}Na_xLa_xTiO_3$ from oxides at 298 K	
$Ca_{1-2x}Na_xLa_xTiO_{3(s,\ 298\ K)} = (1-2x)CaO_{(sln,\ 973\ K)} + 0.5xNa_2O_{(sln,\ 973\ K)} + 0.5xLa_2O_{3(sln,\ 973K)} + TiO_{2(sln,\ 973\ K)}$	$\Delta H_1 = \Delta H_{ds1}$
$CaO_{(s,\ 298\ K)} \rightarrow CaO_{(sln,\ 973\ K)}$	$\Delta H_2 = -90.30 \pm 1.80$ (Navrotsky 2014)
$Na_2O_{(s,\ 298\ K)} \rightarrow Na_2O_{(sln,\ 973\ K)}$	$\Delta H_3 = -217.56 \pm 4.25$ (Tessier et al. 1999)
$La_2O_{3\ (s,\ 298\ K)} \rightarrow La_2O_{3\ (sln,\ 973\ K)}$	$\Delta H_4 = -225.10 \pm 3.16$ (Cheng et al. 2005)
$TiO_{2\ (s,\ 298\ K)} \rightarrow TiO_{2\ (sln,\ 973\ K)}$	$\Delta H_5 = 60.81 \pm 0.11$ (Navrotsky 2014)
$(1-2x)CaO_{(s,\ 298\ K)} + 0.5xNa_2O_{(s,\ 298\ K)} + 0.5x\ La_2O_{3(s,\ 298\ K)} + TiO_{2(s,\ 298\ K)} = Ca_{1-2x}Na_xLa_xTiO_{3(s,\ 298\ K)}$	$\Delta H_6 = \Delta H_{f,ox} = -\Delta H_1 + (1-2x)\Delta H_2 + 0.5x\Delta H_3 + 0.5x\Delta H_4 + \Delta H_5$
(b) Enthalpy of formation of $Ca_{1-2x}Na_xLa_xTiO_3$ from elements at 298 K	
$(1-2x)CaO_{(s,\ 298\ K)} + 0.5xNa_2O_{(s,\ 298\ K)} + 0.5x\ La_2O_{3(s,\ 298\ K)} + TiO_{2(s,\ 298\ K)} = Ca_{1-2x}Na_xLa_xTiO_{3(s,\ 298\ K)}$	$\Delta H_{f,ox}$
$Ca_{(s,\ 298K)} + \frac{1}{2} O_{2(g,\ 298K)} \rightarrow CaO_{(s,\ 298K)}$	$\Delta H_7 = -634.92 \pm 0.90$ (Chase 1998)
$2Na_{(s,\ 298K)} + \frac{1}{2} O_{2(g,\ 298K)} \rightarrow Na_2O_{(s,\ 298K)}$	$\Delta H_8 = -417.98 \pm 4.2$ (Chase 1998)
$2\ La_{(s,\ 298K)} + 3/2O_{2(g,\ 298K)} \rightarrow La_2O_{3(s,\ 298K)}$	$\Delta H_9 = -1791.6 \pm 2$ (Chase 1998)
$Ti_{(s,\ 298K)} + O_{2(g,\ 298K)} \rightarrow TiO_{2(s,\ 298K)}$	$\Delta H_{10} = -944 \pm 0.8$ (Chase 1998)
$(1-2x)Ca_{(s,\ 298\ K)} + xNa_{(s,\ 298\ K)} + xLa_{(s,\ 298\ K)} + Ti_{(s,\ 298\ K)} + 1.5O_{2(g,\ 298\ K)} = Ca_{1-2x}Na_xLa_xTiO_{3\ (s,\ 298\ K)}$	$\Delta H_{f,el\ 298\ K} = (1-2x)\Delta H_7 + 0.5x\Delta H_8 + 0.5x\Delta H_9 + \Delta H_{10}) + \Delta H_{f,ox}$

Table 3. Enthalpies of rare earth perovskites $Ca_{1-2x}Na_xLa_xTiO_3$ ($0 \leq x \leq 0.50$) at 298 K

*Composition **	Chemical Composition	*Tolerance factor*	*x*	$\Delta H_{ds,298K,}$ *kJ/mol***	$\Delta H_{f,ox,298K,}$ *kJ/mol*	$\Delta H_{f,el,298K,}$ *kJ/mol*
$Na_{0.5}La_{0.5}TiO_3$	$Na_{0.495}La_{0.5}TiO_{2.998}$	0.979	0.50	52.645±2.95	-102.5±6.06	-1598.90±7.68
$Ca_{0.25}Na_{0.375}La_{0.375}TiO_3$	$Ca_{0.25}Na_{0.371}La_{0.375}TiO_{2.998}$	0.976	0.375	54.43±3.11	-99.19±6.37	-1616.22±7.98
$Ca_{0.5}Na_{0.25}La_{0.25}TiO_3$	$Ca_{0.5}Na_{0.248}La_{0.25}TiO_{2.999}$	0.972	0.25	56.01±1.66	-95.68±5.83	-1633.34±7.56
$Ca_{0.75}Na_{0.125}La_{0.125}TiO_3$	$Ca_{0.75}Na_{0.124}La_{0.125}TiO_{2.999}$	0.969	0.125	56.89±2.57	-91.47±6.24	-1649.76±7.88
$CaTiO_3$	$CaTiO_3$	0.966	0	56.47±3.92	-85.96±3.92	-1664.88±4.10

*Calculated based on the microprobe analyses from 10 points data for each sample.

** Calculated based on 8 measurements per sample. Uncertainties, calculated as two standard deviations of the mean values, are less than 2%.

Table 4: Energetics of substitutions in loparite minerals *

Solid solutions	Substitution (Oxide Exchange Reaction)	$\Delta H_{f,ox,298K}$, kJ/mol
$CaTiO_3$ - $NaNbO_3$	$Ca_A^{2+}+Ti_B^{4+} \leftrightarrow Na_A^{+} + Nb_B^{5+}$ ($CaTiO_3 + 0.5Na_2O + 0.5Nb_2O_5$ $= NaNbO_3 + CaO+TiO_2$)	-71.4 ± 4.5
$CaTiO_3$ - $SrTiO_3$	$Ca_A^{2+} \leftrightarrow Sr_A^{2+}$ ($CaTiO_3 + SrO = SrTiO_3 + CaO$)	-31.1±4.4
$CaTiO_3$ - $Na_{0.5}La_{0.5}TiO_3$	$Ca_A^{2+} \leftrightarrow 0.5Na_A^{+} + 0.5\ La_A^{3+}$ ($CaTiO_3 + 0.25Na_2O + 0.25La_2O_3$ $= Na_{0.5}La_{0.5}TiO_3 + CaO$)	-16.0±7.2
$SrTiO_3$ - $NaNbO_3$	$Sr_A^{2+}+Ti_B^{4+} \leftrightarrow Na_A^{+} + Nb_B^{5+}$ ($SrTiO_3 + 0.5Na_2O + 0.5Nb_2O_5$ $= NaNbO_3 + SrO+TiO_2$)	-40.3±3.0
$Na_{0.5}La_{0.5}TiO_3$ - $NaNbO_3$	$0.5La_A^{3+}+Ti_B^{4+} \leftrightarrow 0.5Na_A^{+} + Nb_B^{5+}$ ($Na_{0.5}La_{0.5}TiO_3 + 0.5Nb_2O_5 + 0.25Na_2O$ $= NaNbO_3 + 0.25La_2O_3 + TiO_2$)	-55.4±6.4
$SrTiO_3$ - $Na_{0.5}La_{0.5}TiO_3$	$Sr_A^{2} \leftrightarrow 0.5Na_A^{+} + 0.5La_A^{3+}$ ($SrTiO_3 + 0.25Na_2O + 0.25La_2O_3$ $= Na_{0.5}La_{0.5}TiO_3 + SrO$)	15.1±6.4

- Calculated from differences in formation enthalpies of the perovskites from the oxides as discussed in text. Values from this work and Xu et al. (2005)

Figure Captions

Figure. 1 Compositional relationships of naturally occurring loparite solid solution in quaternary system perovskite ($CaTiO_3$) - lueshite ($NaNbO_3$) - tausonite ($SrTiO_3$) - loparite ($Na_{1/2}Ln_{1/2}TiO_3$) (*Ln* =La, Ce, Pr, Nd)

Figure. 2 Crystal Structure of $Ca_{1-2x}Na_xLa_xTiO_3$ ($0 \leq x \leq 0.50$) end members – $La_{0.5}Na_{0.5}TiO_3$ (tetragonal) and $CaTiO_3$ (orthorhombic)

Figure 3. X-ray diffraction data and calculated pattern for $Ca_{1-2x}Na_xLa_xTiO_3$ ($0 \leq x \leq 0.50$). The experimental data are shown as crosses, the calculated fits and difference curves as solid lines.

Figure 4. Lattice parameters (a, b, c) as a function of composition in $Ca_{1-2x}Na_xLa_xTiO_3$, ($0 \leq x \leq 0.50$)

Figure 5. Drop solution enthalpy as a function of composition in $Ca_{1-2x}Na_xLa_xTiO_3$ ($0 \leq x \leq 0.50$), where the dashed vertical line indicates the phase transition

Figure 6: Formation enthalpy of $Ca_{1-2x}Na_xLa_xTiO_3$ as a function of (a) Na+La substitution and (b) Goldschmidt tolerance factor.

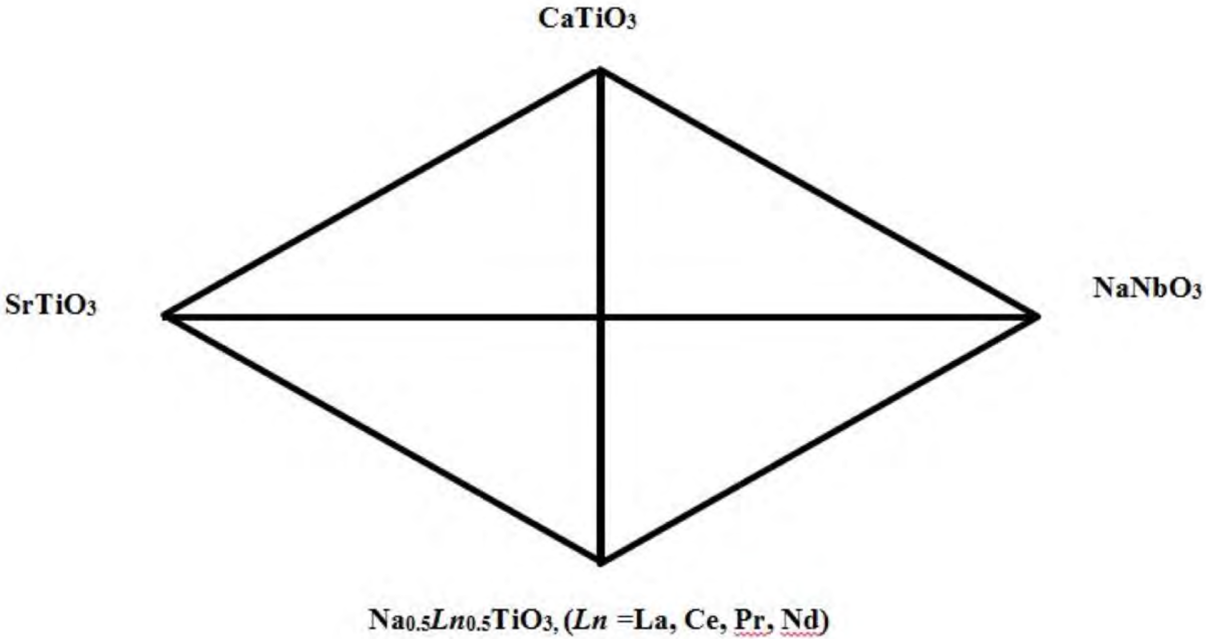
$CaTiO_3$
$SrTiO_3$
$NaNbO_3$
$Na_{0.5}Ln_{0.5}TiO_3$, (Ln =La, Ce, Pr, Nd)

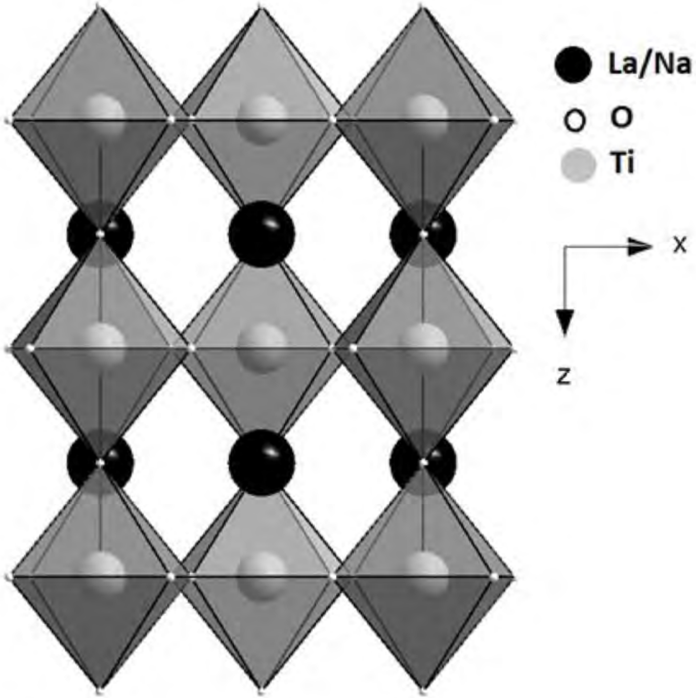
La/Na
O
Ti
x
z

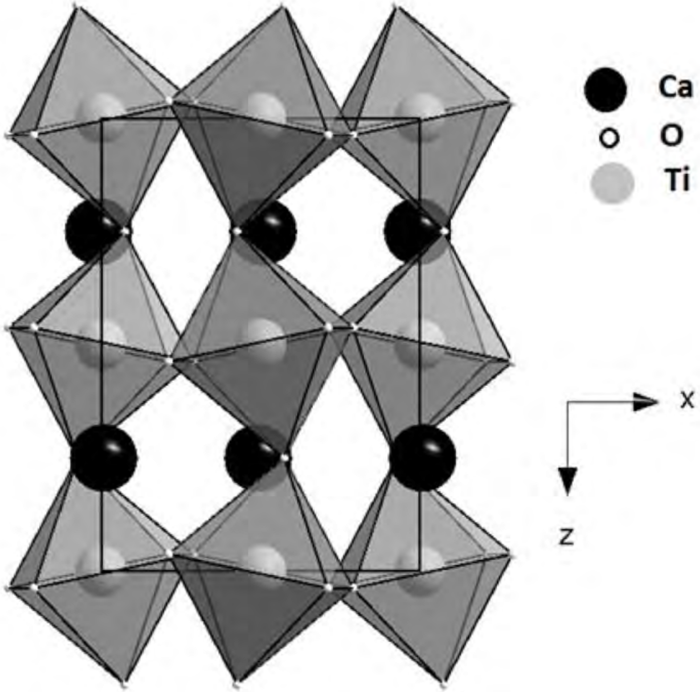
Ca
O
Ti
x
z

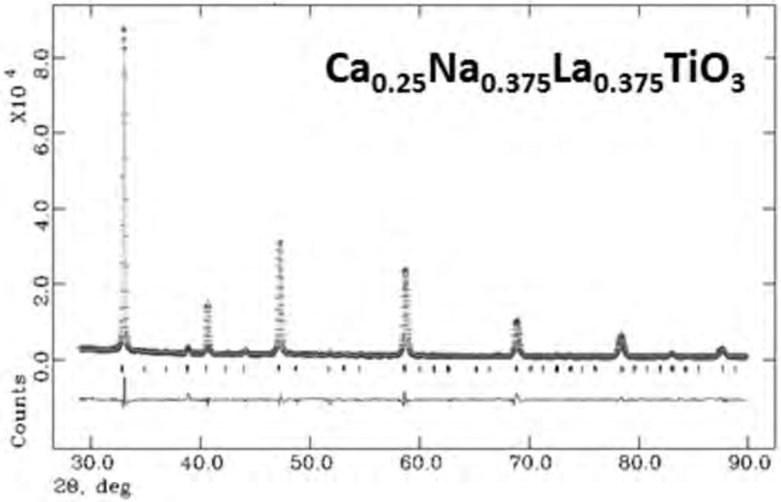
$Ca_{0.25}Na_{0.375}La_{0.375}TiO_3$
X10 ^{4}
8.0
6.0
4.0
2.0
0.0
Counts
30.0
40.0
50.0
60.0
70.0
80.0
90.0
2θ, deg

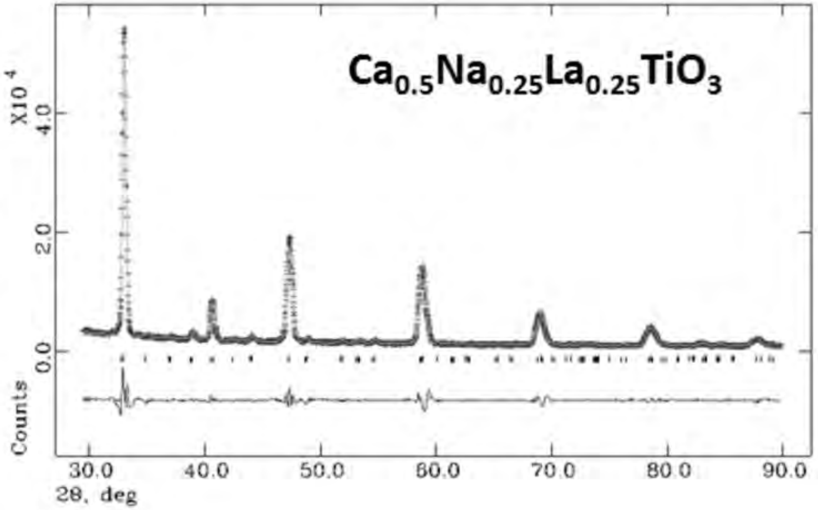
$Ca_{0.5}Na_{0.25}La_{0.25}TiO_3$
X10 ^{4}
4.0
2.0
0.0
Counts
30.0
40.0
50.0
60.0
70.0
80.0
90.0
2θ, deg

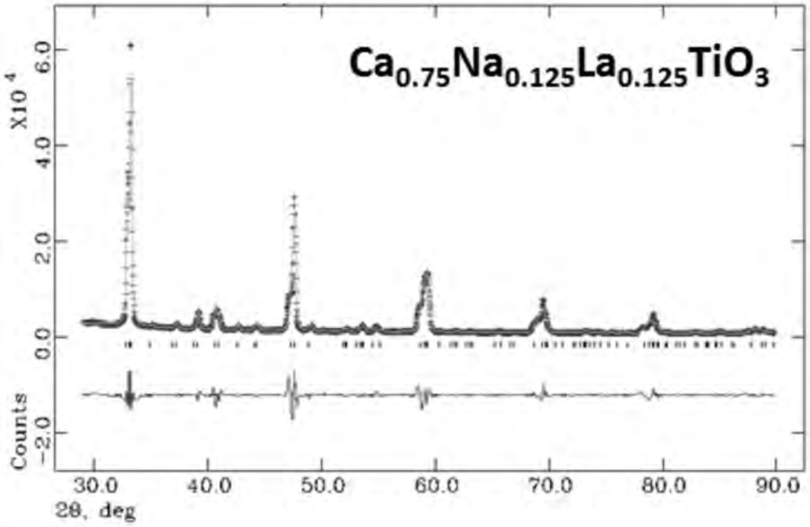
$Ca_{0.75}Na_{0.125}La_{0.125}TiO_3$
X10 ^{4}
6.0
4.0
2.0
0.0
-2.0
Counts
30.0
40.0
50.0
60.0
70.0
80.0
90.0
2θ, deg

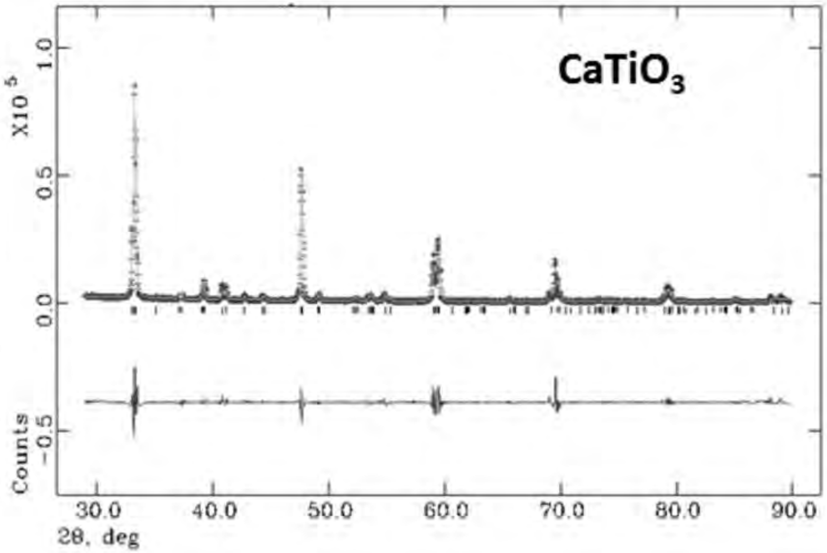
$CaTiO_3$
X10 ^{5}
1.0
0.5
0.0
-0.5
Counts
30.0
40.0
50.0
60.0
70.0
80.0
90.0
2θ, deg

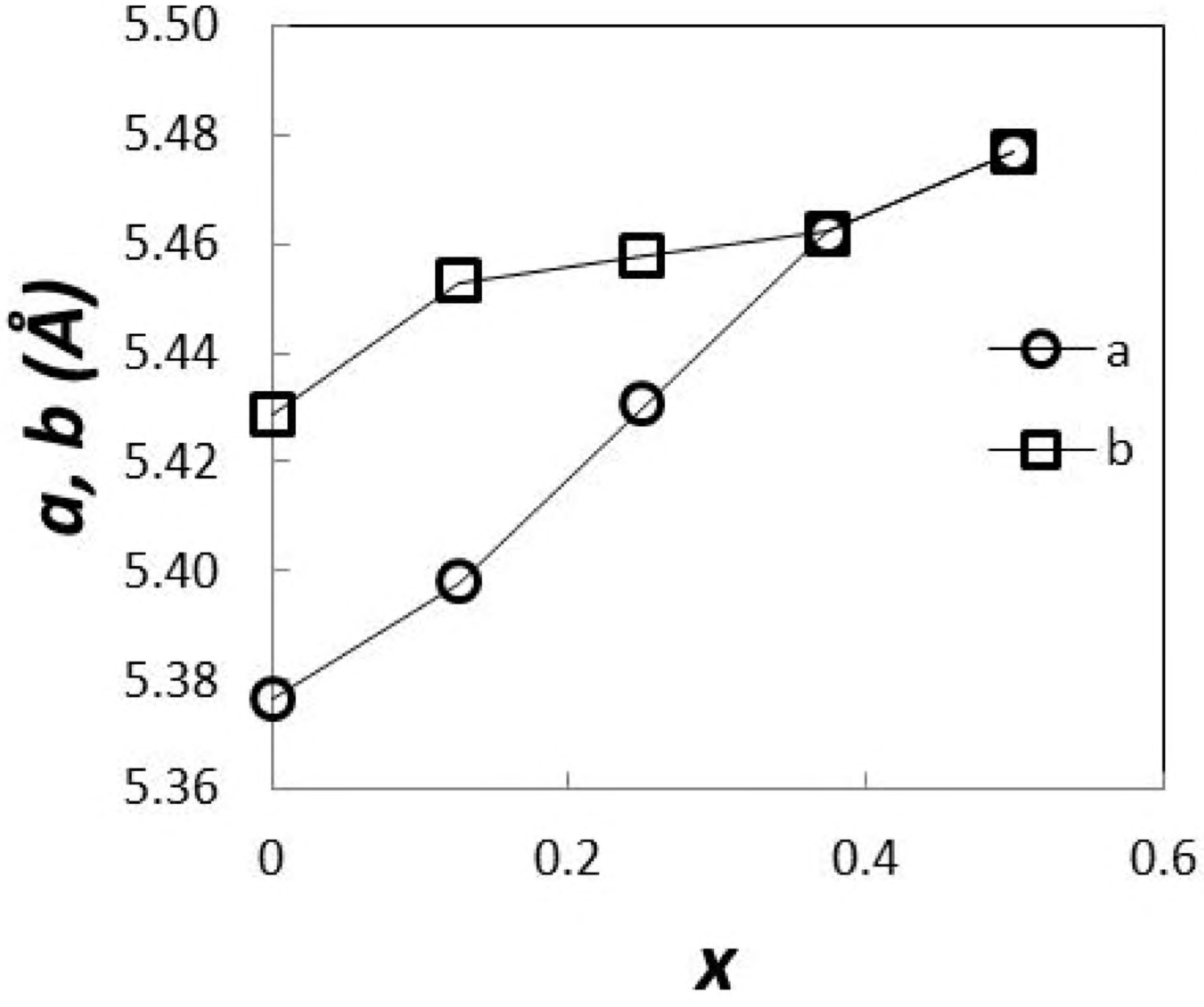
a, b (Å)
5.50
5.48
5.46
5.44
5.42
5.40
5.38
5.36
0
0.2
0.4
0.6
x
a
b

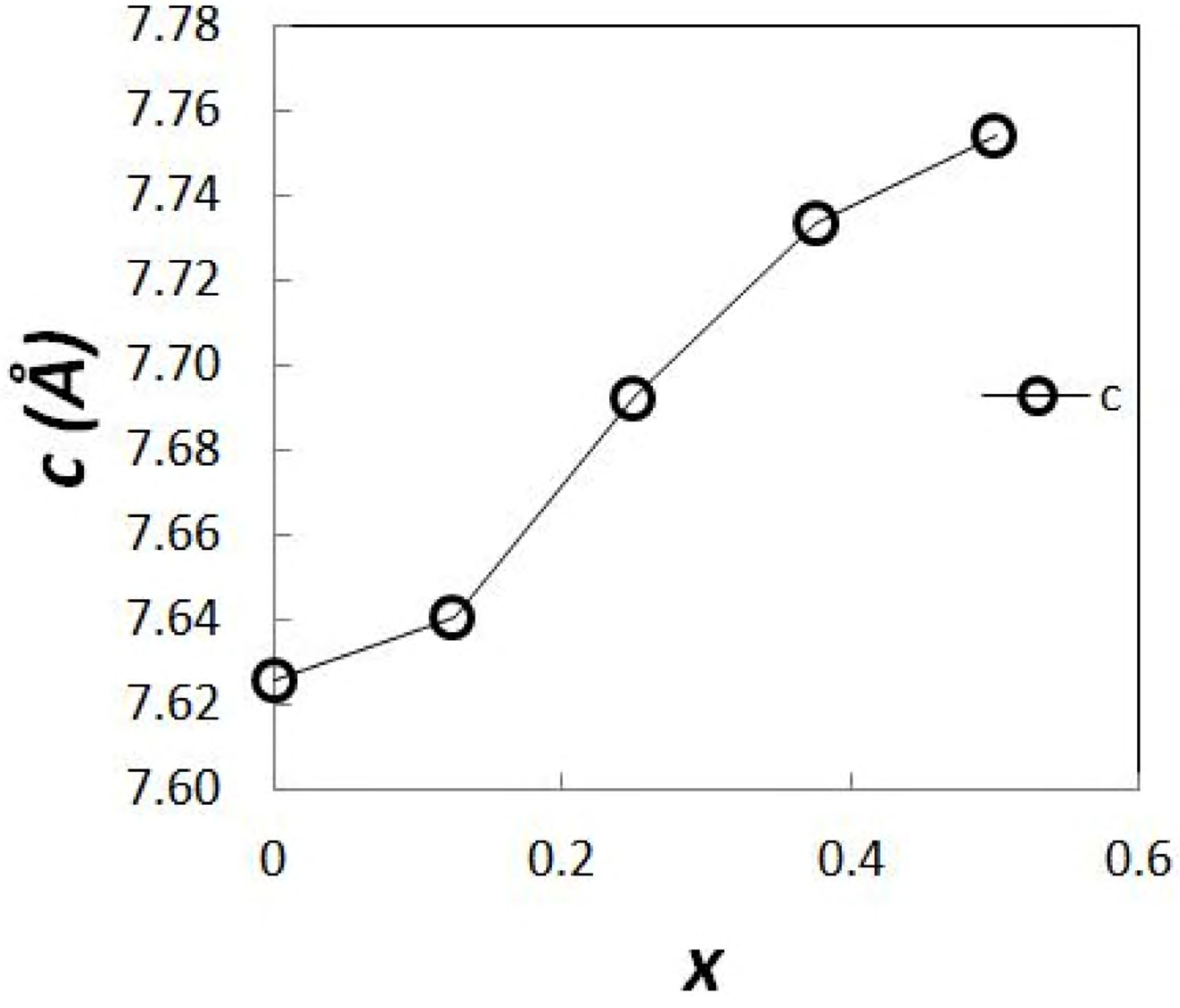
c (Å)
7.78
7.76
7.74
7.72
7.70
7.68
7.66
7.64
7.62
7.60
0
0.2
0.4
0.6
x
c

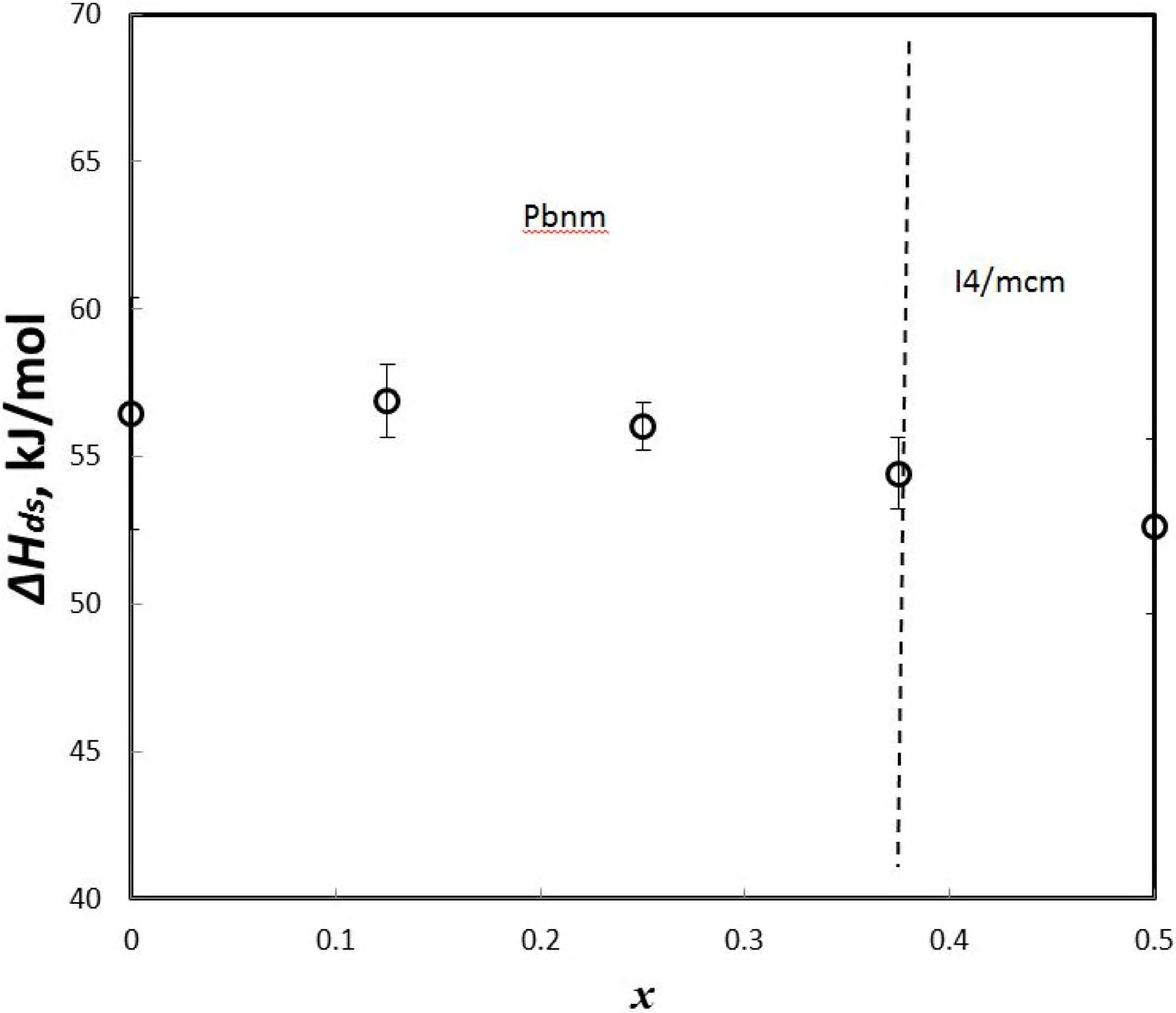
70
65
60
55
50
45
40
0
0.1
0.2
0.3
0.4
0.5
ΔH_ds, kJ/mol
x
Pbnm
I4/mcm

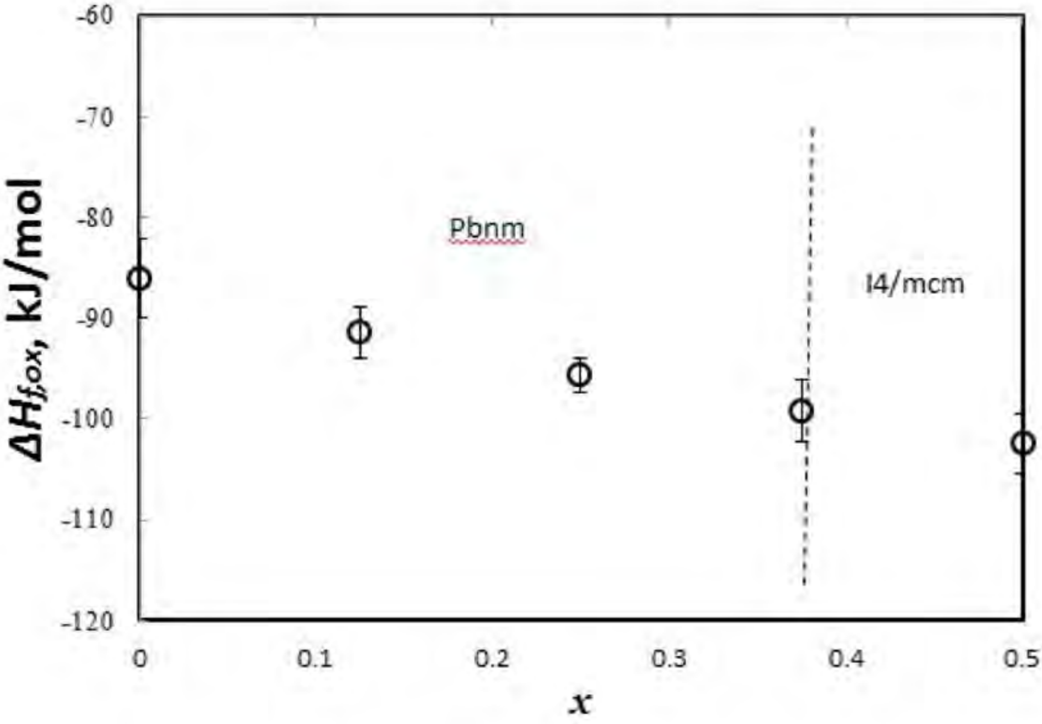
-60
-70
-80
-90
-100
-110
-120
ΔH_f,ox, kJ/mol
Pbnm
I4/mcm
0
0.1
0.2
0.3
0.4
0.5
x

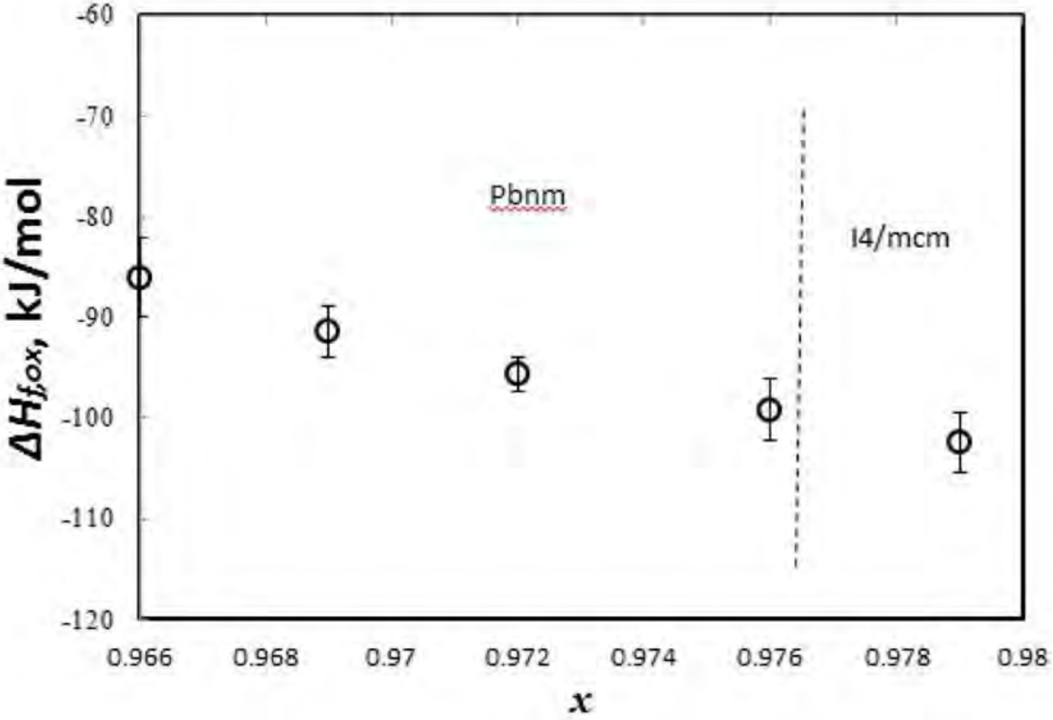
-60
-70
-80
-90
-100
-110
-120
ΔH_f,ox, kJ/mol
Pbnm
I4/mcm
0.966
0.968
0.97
0.972
0.974
0.976
0.978
0.98
x